University of Groningen

The monthly dynamics of blue water footprints and electricity generation of four types of hydropower plants in Ecuador

Vaca Jiménez, Santiago; Gerbens-Leenes, P.W.; Nonhebel, Sanderine

IMPORTANT NOTE: You are advised to consult the publisher's version (publisher's PDF) if you wish to cite from it. Please check the document version below.

Document Version
Publisher's PDF, also known as Version of record

[Link to publication in University of Groningen/UMCG research database](#)

The monthly dynamics of blue water footprints and electricity generation of four types of hydropower plants in Ecuador

S. Vaca-Jiménez [a,b,*], P.W. Gerbens-Leenes [a], S. Nonhebel [a]

[a] Center for Energy and Environmental Sciences, University of Groningen, 9747 AG Groningen, the Netherlands
[b] Escuela Politécnica Nacional, Ladrón de Guevera, E11-253 Quito, Ecuador

HIGHLIGHTS

- The evaporation and open water surfaces of hydropower plants have daily variation.
- Static open water surface approaches have under and overestimated evaporation.
- Climate, reservoir's size, storage, and electricity output define WFs of hydropower.
- Plants with *flooded rivers* and large *gross static heads* are most water-efficient.
- Plants with small WFs are not the best option from a water and energy perspective.

GRAPHICAL ABSTRACT
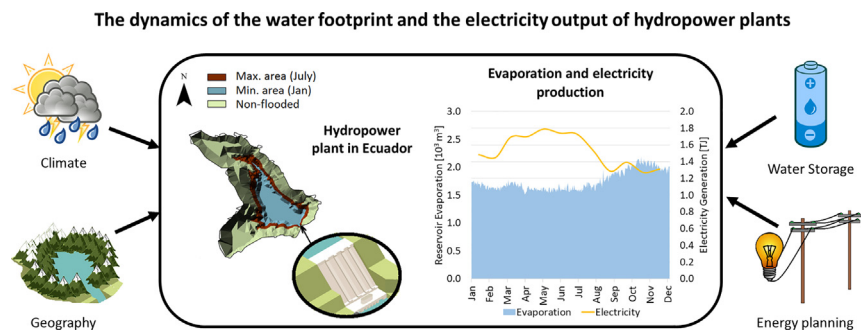
ARTICLE INFO

ABSTRACT

Water evaporates from reservoirs of hydropower plants (HPPs), often in significant volumes. Reservoir evaporation is a dynamic phenomenon depending on climate, varying size of open water surfaces (OWS), and electricity production. Due to a lack of data and methods to estimate the OWS's size variation, previous studies assessed HPPs water footprints (WFs) considering static OWSs acknowledging the uncertainty of this omission. This study estimates WFs of HPPs, considering dynamic OWSs for four plant types in Ecuador, *Flooded lakes*, and *Flooded rivers*, with dam heights lower or higher than their *Gross Static Head* (GSH). It quantifies OWSs size variation using a Digital Elevation Model and GSH data, assessing OWS evaporation, effects on electricity production and WFs. There are large differences among the evaporation of HPPs when OWS size variations are considered. HPP operation, geographical features, and climate determine temporal differences. *Flooded lake* HPPs have relatively large WFs. *Flooded River* HPPs, with dam heights below their GSH, have the smallest WFs, but water storage capacity is limited. Static area approaches underestimated annual WFs by 10% (*Flooded Lake* HPPs) to 80% (*Flooded River* HPPs). Earlier studies showed effects of HPPs on water from a water management perspective, suggesting that less water-intensive HPP technologies are favorable, or that other water-efficient electricity-generating technologies, like solar or wind, should replace HPPs. This study also included the electricity perspective, indicating that energy management and water storage are important factors for WFs. The most water-effective technology cannot fulfill current electricity production due to a lack of storage options. The system dynamics analysis indicates that aiming for small WFs is not always the best option from an energy and water perspective.

* Corresponding author at: Escuela Politécnica Nacional, Ladrón de Guevera, E11-253 Quito, Ecuador.
  E-mail address: santiago.vaca@epn.edu.ec (S. Vaca-Jiménez).

1. Introduction

Hydropower plants (HPPs) consume freshwater due to evaporation from the surface of their reservoirs (Gleick, 1992; Mekonnen and Hoekstra, 2012). The water volume evaporated per unit of electricity is larger than for most of the other renewable and non-renewable electricity generating technologies (except biomass) (Gleick, 1994; Mekonnen et al., 2016; Vaca-Jiménez et al., 2019a). As the global electricity mix is transitioning from fossil to renewable energy sources to reduce GHG emissions, hydropower is likely to become the largest renewable technology deployed globally (IEA, 2016). Thus, a tradeoff appears as the new global electricity mix is low in carbon emissions, but significantly more water-intensive (Mekonnen et al., 2016). This can be problematic in a water-constrained world.

The publication of Gleick (1992) on energy and water relationships was the start of many studies assessing water consumption by hydropower plants (HPPs). Most studies have focused on the water perspective, showing the effect of HPP reservoirs on the hydrosphere. Key studies include Bakken et al. (2016a, 2016b), Coelho et al. (2017), Grubert (2016), Herath et al. (2011), Hogeboom et al. (2018), Liu et al. (2015), Mekonnen and Hoekstra (2012), and Scherer and Pfister (2016). Those studies have used different datasets, case studies, and methods. They have all considered evaporation as the main factor of HPP water consumption.

Reservoir evaporation is a dynamic phenomenon, which depends on the variation of the open water surface (OWS) area and temporal climate variation. Moreover, HPP electricity generation varies in time, constrained by energy management and dependent on electricity mix dynamics and physical variables. In a specific mix, often, some power plants are prioritized over others (Egré and Milewski, 2002; Vaca-Jiménez et al., 2019b). Physical variables that influence electricity generation are, for example, the size of the water flows passing the turbines and reservoir water level heights (Gross Static Head, GSH). These two variables are related and climate-dependent, showing temporal variation. For instance, precipitation variation translates into variations of river flows, surface sizes and GSH's, affecting electricity production (Gleick, 1992). Additionally, a HPP system often has a feedback loop, as electricity production also affects reservoir characteristics. For instance, more electricity production with faster turbine flow rates decreases reservoir water volumes (Cai et al., 2018). Decreased water volumes translate into lower heads and smaller electricity output. Hence, HPP water consumption is part of a dynamic process influenced by interlinked variables, e.g., evaporation rates, open water surface areas and electricity production.

So far, research has not considered process dynamics, like reservoir surface size variation, assuming a constant surface area (a *constant approach*). Several studies have estimated these surface areas using different data sources. For instance, Hogeboom et al. (2018) and Scherer and Pfister (2016) have used data from global databases as the Global Reservoir and dam databases (GRanD) (Lehner et al., 2011), or the World Register of Dams (WRD) (ICOLD, 2018). Others, e.g., Herath et al. (2011) and Vaca-Jiménez et al. (2019a), have used approximated measurements using Geographic Information Systems (GIS). All studies have considered a static OWS due to a lack of data on size variation and the large scope that they covered (most of them assessed a large range of HPPs). However, most studies emphasize that excluding OWS size variation leads to uncertainty of water consumption values because reservoir evaporation might be over or underestimated (Bakken et al., 2013; Hogeboom et al., 2018; Mekonnen and Hoekstra, 2012). They recommend additional, more detailed case studies that include OWS size variation.

Our previous work has quantified the WF of Ecuadorian electricity technologies (Vaca-Jiménez et al., 2019a), showing how technology operation dynamics affect temporal and spatial WF variation of an electricity mix (Vaca-Jiménez et al., 2019b). However, those studies used the *constant approach* assuming the HPP OWS size remains the same. This study is a continuation of our earlier work, including system dynamics of HPPs in which OWS size variation influences WFs. Using previous work, we focused on a smaller case study with more detail taking temporal variation into account.

Ecuador is a water-abundant country with large hydropower potential. HPPs are the largest contributors to the country's electricity mix (MEER, 2017). However, their electricity output decreases seasonally when river water is limited. There are many HPPs with different infrastructure, capacity, and technology, for example, HPPs with reservoirs that form *Flooded Lakes* or *Flooded Rivers* (Vaca-Jiménez et al., 2019a), and HPPs with a dam height (DH) larger or smaller than the *GSH*. This study aims to estimate the WF of HPPs, considering the dynamics of the hydropower system for four types of HPPs based on different reservoir types and *DH-GSH* relations.

This study answers the following research questions: (i) How much does reservoir evaporation of four Ecuadorian HPPs types change through the year due to temporal climate and reservoir size variation? (ii) What is the temporal variation of the WF and electricity production of the four types of Ecuadorian HPPs? And how does this variation affect their annual WF? (iii) What can we learn from the dynamics between electricity generation, water storage (reservoir size), and climate of these four HPPs? And (iv) what are the implications for the electricity system and its WF when the most water-efficient technology is scaled-up to replace the existing electricity generating infrastructure in Ecuador?

2. System description

Evaporation from HPP OWSs depends on three factors: (i) HPP technology; (ii) geographical features of the site where the HPP is located; and (iii) climate. Factor (i) defines electricity output, while factors (ii) and (iii) determine the OWS shape and water evaporation rates.

2.1. Hydropower plant technologies and classification

Based on the OWS size and shape, HPPs can be classified into three groups: (i) *Dammed* HPPs, which impound water before a dam, usually having large reservoirs; (ii) *run-of-the-river* HPPs (ROR), which divert river flows by a weir, which is smaller than a dam. They usually do not create large reservoirs, but ponds without significant temporal OWS size variation, and (iii) *In-conduit* HPPs, in which small HPPs are located in-between water supply pipelines. These HPPs do not have OWSs. Previous studies have shown that *dammed* HPPs have the largest WFs (Liu et al., 2015; Vaca-Jiménez et al., 2019a).

Dammed HPPs include two subgroups, depending on the powerhouse position in relation to the *DH*: (i) HPPs with powerhouses at the bottom of the dam. The *DH* is larger than the *GSH* ($DH > GSH$); and (ii) HPPs with large penstocks that conduct water into powerhouses below the dam's bottom. The *DH* is smaller than the *GSH* ($DH < GSH$) (Gleick, 1994, 1992). Usually, $DH > GSH$ HPPs have larger evaporative losses per unit of electricity output, as they produce less electricity than comparable $DH < GSH$ HPPs (Gleick, 1994). *Dammed* HPPs can also be classified based on their OWS shape. Vaca-Jiménez et al. (2019a) classified them into (i) HPPs with OWSs with long, wide, and shallow flooded areas (*Flooded Lakes*); and (ii) HPPs with OWSs with long, narrow and deep flooded areas (*Flooded Rivers*). HPPs with *Flooded Rivers* have smaller WFs than *Flooded Lakes*, because, generally, *Flooded Rivers* have smaller flooded areas than *Flooded Lakes* per unit of electricity produced (Gleick, 1994; Liu et al., 2015; Vaca-Jiménez et al., 2019b). There are four *dammed* HPP groups using these two classification criteria: (i) $DH > GSH$ - *Flooded Lake*, (ii) $DH > GSH$ - *Flooded River*, (iii) $DH < GSH$ - *Flooded Lakes*, and (iv) $DH < GSH$ - *Flooded River*.

2.2. Geography

Ecuador, located in South America, is divided into two parts by the Andes mountains from north to south. Rivers flow from the top of the Andes to the two major basins: the Pacific (west of the Andes) and the Amazon basin (east of the Andes) (SENAGUA, 2002). HPPs are built in the Andes' highlands, lowlands, and in between them. The HPP OWSs in the highlands are usually *Flooded Lakes*; the HPP OWSs in between highlands and lowlands *Flooded Rivers* (Vaca-Jiménez et al., 2019a).

2.3. Climate

Ecuador's geography causes different climates so that the two basins have different weather conditions and freshwater availability. Ecuador has two seasons: a dry and a wet season. The Amazon basin has 88% of Ecuador's freshwater resources (CEPAL, 2010), but the difference between wet and dry seasons is smaller than in the Pacific. Reservoirs in the Amazon basin have smaller volumetric fluctuations than reservoirs in the Pacific basin as river water volumes are relatively constant (Vaca-Jiménez et al., 2019b).

For both basins, there is a distinction between the climate of the highlands and the lowlands. The Ecuadorian highlands have dry temperate climates; the lowlands humid tropical climates (INAMHI, 2018; Rollenbeck and Bendix, 2011). HPP reservoirs in the highlands have smaller evaporation rates than reservoirs in the lowlands because temperature and solar radiation are smaller.

2.4. Composition of the Ecuadorian electricity mix and its dynamics

The Ecuadorian electricity mix includes hydropower, thermal, biomass, solar (PV), wind, and biogas power plants. 97% of Ecuadorian electricity is produced by HPPs and thermal power plants (*TPPs*), using crude oil derivatives (ARCONEL, 2018). HPPs are the largest electricity producers (MEER, 2017). Their output increases during the wet season when river water volumes are relatively large and decreases during the dry season. This variation affects the overall electricity production. In 2017, Ecuadorian HPPs had a capacity factor of 51% (ARCONEL, 2018), which is smaller than the average 54% of the region (Kumar et al., 2011). During the dry season, *TPPs* serve as a backup of HPPs, increasing their production to fulfill electricity demand.

3. Method

The water footprint (WF) method is a tool that estimates freshwater volumes consumed by humans (Hoekstra et al., 2011), for example, water to produce electricity by hydropower (Mekonnen and Hoekstra, 2012). Theoretically, the WF of a HPP includes a direct and indirect WF. The direct WF is the blue water that evaporates from the OWS. The indirect WF considers HPP construction and decommissioning (Vaca-Jiménez et al., 2019a). Some studies, e.g., Hogeboom et al. (2018) and Mekonnen et al. (2015), have shown that WFs of the construction and decommissioning phases are negligible compared to the direct WF caused by OWS evaporation. Therefore, we assumed that the indirect WF is negligible.

The assessment of the hydropower WF in Ecuador included five clusters of steps: (i) the estimation of temporal variation of OWSs sizes per HPP (*steps 1–3*); (ii) the calculation of daily OWS evaporation rate per HPP (*steps 4–5*); (iii) the calculation of HPP WFs (*steps 6–9*); (iv) the analysis of variable dynamics affecting HPP WFs (*steps 10–11*), which includes the dynamics of the relationship between evaporation rates, OWS area sizes and storage, the effect on electricity production, and the HPP WFs (m^3/TJ and $m^3/month$); and (v) the assessment of impacts on the electricity system and blue WF when the most-water efficient technology replaces current technologies (*steps 12–19*). Fig. 1 shows the calculation steps and how they relate to each other.

3.1. Case studies

Based on the *DH-GSH* relation and the OWS shape, we identified four HPP groups in Ecuador. For each group, we selected a HPP that represents the group: Marcel Laniado, Mazar, Paute, and Saucay. Marcel Laniado (213 MW) with *DH* > *GSH* HPP is located in the Pacific basin lowlands (CELEC EP - Hidronación, 2018). Its OWS is the largest in Ecuador, forming a long and wide *Flooded Lake*, flooding 30,000 ha of land (Lehner et al., 2011). Mazar (170 MW) with *DH* > *GSH* is located in the Andes in the Amazon basin (CELEC EP - Hidropaute, 2018). Its OWS is a long and narrow *Flooded River* with a reservoir constrained by mountains. Paute (1075 MW), nearby Mazar (CELEC EP - Hidropaute, 2018), has a *DH* < *GSH* and an OWS forming a long and narrow *Flooded River*. Saucay (24 MW), with a *DH* < *GSH*, is located in the highlands of the Amazon basin (Elecaustro, 2018). It has two reservoirs that form *Flooded Lakes*: (i) Chanlud and (ii) El Labrado. During the wet season, Marcel Laniado and Mazar's OWSs store water for over a month (CELEC EP - Hidronación, 2013; CELEC EP - Hidropaute, 2018), while Paute and Saucay's OWSs store water for only a few days (CELEC EP - Hidropaute, 2018; Elecaustro, 2018). Table 1 summarizes the characteristics and OWSs of the four HPPs considered in this study.

3.2. Estimation of temporal variation of Open Water Surface size

Power companies and dam managers usually measure and record reservoir *GSH*s. The OWS size is seldom measured because it is irrelevant for HPP operation. Without data, OWS size variation needs to be estimated. The OWSs usually flood natural landscapes, which are seldom geometrical or have parallel features, covering large land areas that vary in altitude and depth, impeding the use of geometric approximations. HPP operators use *GSH* data to control reservoir water levels and estimate potential electricity generation. There is a relation between *GSH* and OWS's size variation (see Fig. 2), but the relation is not linear because the reservoir's shapes vary. Snyder et al. (2013) have made risk assessments of places subject to flooding using topographical information to create a 3D terrain model, a Digital Elevation Model (DEM). We adopted this approach for the OWS size estimation considering the topographical information of the flooded area. When coupled with daily historical *GSH* data, the DEM model estimates OWS size changes. We applied the approach for the four HPP cases.

Step 1 created the DEM of HPP OWSs using ArcGIS, ArcMap 10® and topographical terrain information from IGM (2018). *Appendix A* gives the method used for the creation of the DEM.

Step 2 estimated the flooded area per day *d* of OWS *r*, $A_d[r]$ (ha), using daily *GSH* data of OWS *r* as the elevation input of the *Surface Volume* tool of ArcGIS, ArcMap 10®. *GSH* data for 2003–2018 for Mazar and Paute HPPs were derived from CELEC EP - Hidropaute (2018). For Marcel Laniado, data for 2008–2014 were derived from CELEC EP - Hidronación (2014), and for Saucay, data from 2008 to 2018 were provided by the operator (Elecaustro, 2018). *Appendix B* gives the HPP *GSH* data.

Finally, **Step 3** compared the $A_d[r]$ of OWS *r* to the area reported in the GRanD database (Lehner et al., 2011) and in Vaca-Jiménez et al. (2019a), who measured Ecuadorian HPP OWS areas using satellite imaging and ArcGIS®.

3.3. Calculation of daily evaporation from hydropower open water surfaces

To calculate OWS daily evaporation rates, we used the Modified Penman method (Harwell, 2012) that has also been used for similar studies, e.g., Hogeboom et al. (2018), Mekonnen and Hoekstra (2012) and Vaca-Jiménez et al. (2019a). It is effective to estimate OWS evaporation in tropical regions (Coelho et al., 2018).

First, **Step 4** located HPPs and related OWS from Vaca-Jiménez et al. (2019a). Next, **Step 5** calculated OWS daily evaporation rates, $Ev_d[r]$
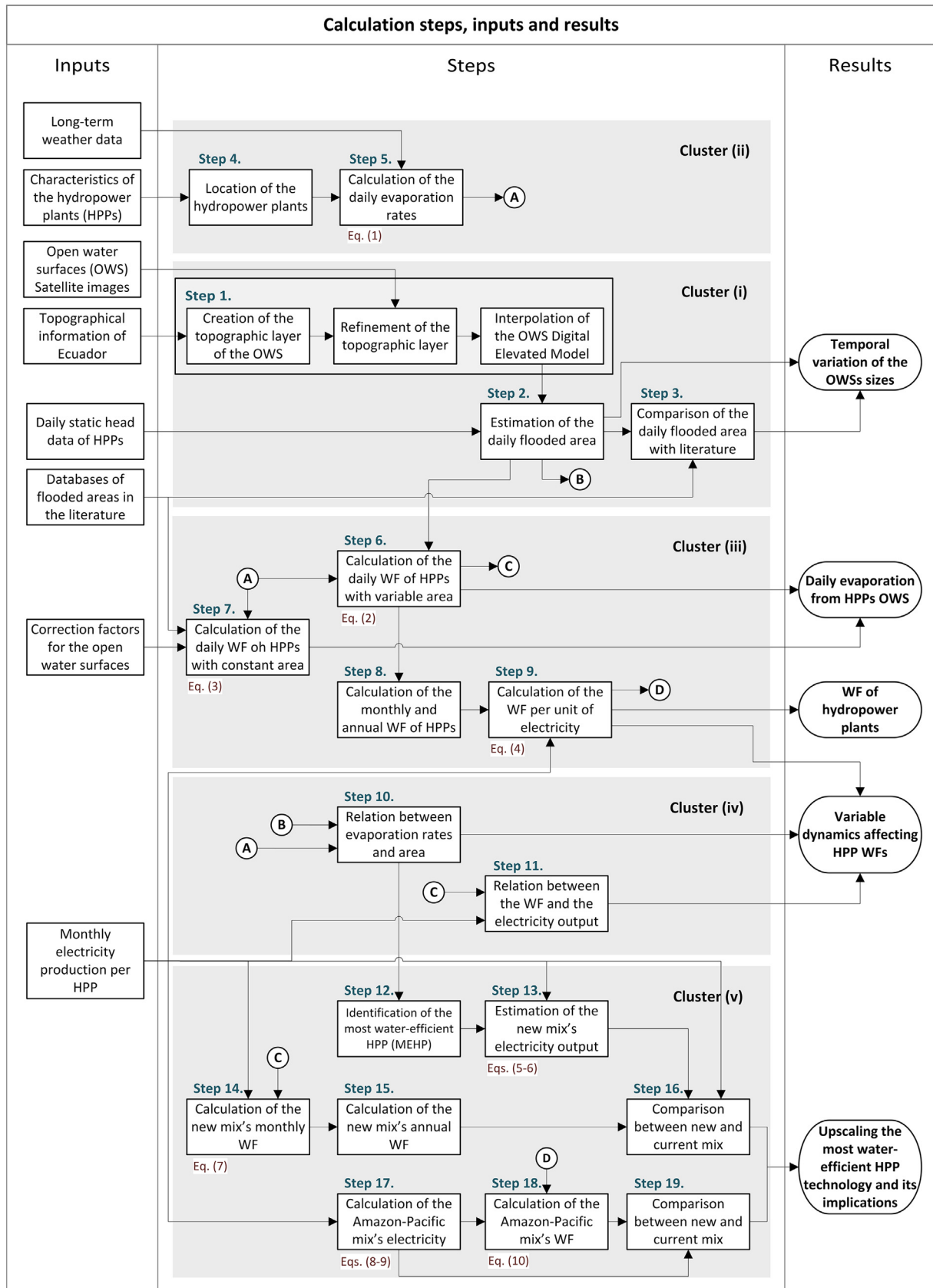
Calculation steps, inputs and results

Inputs	Steps	Results

Fig. 1. Calculation steps, in four clusters, and their relation to each other.

Table 1
Characteristics of the four hydropower plants considered in this study and their open water surfaces.

Hydropower plant				Open Water Surface			
Name	Capacity [MW][a]	Altitude [masl]	Type	Name	Maximum area [ha]		Shape[d]
					GIS[b]	GRanD[c]	
Marcel Laniado	213	88	DH > GSH	Daule-Peripa	29,500	30,000	Flooded lake
Mazar	170	2155	DH > GSH	Mazar	737	446	Flooded river
Paute	1075	1990	DH < GSH	D. Palacios	256	202	Flooded river
Saucay[e]	24	3470	DH < GSH	Chanlud	66.3	–	Flooded lake
				El Labrado	61.7	–	Flooded lake

[a] Data derived from ARCONEL (2019).
[b] Refers to the area measurement based on Geographical Information System analysis, using satellite imaging. Data derived from Vaca-Jiménez et al. (2019a).
[c] Data derived from the Global reservoir and dam database (GRanD) Database (Lehner et al., 2011).
[d] Based on the classification made by Vaca-Jiménez et al. (2019a).
[e] Saucay has two reservoirs, Chanlud, and El Labrado.

(mm/day), as:

$$Ev_d[r] = 0.7 \left(\frac{\Delta}{\Delta + \gamma} R_n + \frac{\gamma}{\Delta + \gamma} E_a \right) \tag{1}$$

where R_n is the effective net radiation (mm/day), E_a is the theoretical evaporation from a Class A pan (mm/day), Δ is the saturated vapor pressure gradient, and γ is the psychrometric constant. These variables are calculated using long-term average daily climate data, e.g., air temperature, dew point temperature, relative humidity, evaporation rate from a Class A pan, wind speed, and solar radiation. *Appendix C* gives the equations to calculate these variables. We used data of weather stations near the HPPs from INAMHI (2019) and solar radiation data from CONELEC (2008). The selection method of the stations was adopted from Vaca-Jiménez et al. (2019a), who paired stations and HPPs based on proximity and similar climatic conditions.

3.4. Calculation of water footprints of hydropower plants

For the calculation of HPP WFs, we used the *Gross Method* adopted from Mekonnen and Hoekstra (2012). **Step 6** calculated HPP WFs per day d, $WF_d[p]$ (m³/day), considering OWS area variation as:

$$WF_d[p] = \sum_{r=1}^{R} (10 * Ev_d[r] * A_d[r]) \tag{2}$$

where the factor 10 is used to convert mm to m³/ha, $Ev_d[r]$ is the daily evaporation (mm) of OWS r of day d and $A_d[r]$ is the OWS *area* r (ha) on day d. $Ev_d[r]$ and $A_d[r]$ are dynamic and vary in time. Some HPPs have two or more OWSs. For those cases, $WF_{OWS}[p]$ was calculated by summing OWS's evaporation.

For comparison, we also calculated HPP WFs using the *constant approach*. **Step 7** calculated HPP WFs based on Hogeboom et al. (2018), $WF_h[p]$ (m³) as:

$$WF_{h,d}[p] = \sum_{r=1}^{R} (10 * Ev_d[r] * A_{max}[r] * k) \tag{3}$$

where $A_{max}[r]$ is the maximum reported OWS r area, assumed constant throughout the year, and k is a correction factor to avoid OWS evaporation overestimation. Hogeboom et al. (2018) assumed the OWS is half-full most of the time, using a value of 0.5625 for k. Data on HPP OWS size were derived from the GRanD database (Lehner et al., 2011).

Step 8 calculated monthly and annual WFs, $WF_m[p]$ and $WF_y[p]$ (m³), per HPP p by aggregating $WF_d[p]$ per month m, next aggregating $WF_m[p]$ to a year.

Step 9 calculated monthly and annual WFs per unit of electricity, $WF_{m,\,e}[p]$ and $WF_{y,\,e}[p]$ (m³/TJ) as:

$$WF_{m,e}[p] = \frac{WF_m[p]}{E_m[p]}$$

$$WF_{y,e}[p] = \frac{WF_y[p]}{E_y[p]} \tag{4}$$

where $E_m[p]$ is the multiannual average of electricity produced per month m, and $E_y[p]$ is the annual average of electricity produced (TJ) per HPP p. Data on $E_m[p]$ and $E_y[p]$ were derived from Vaca-Jiménez et al. (2019b).
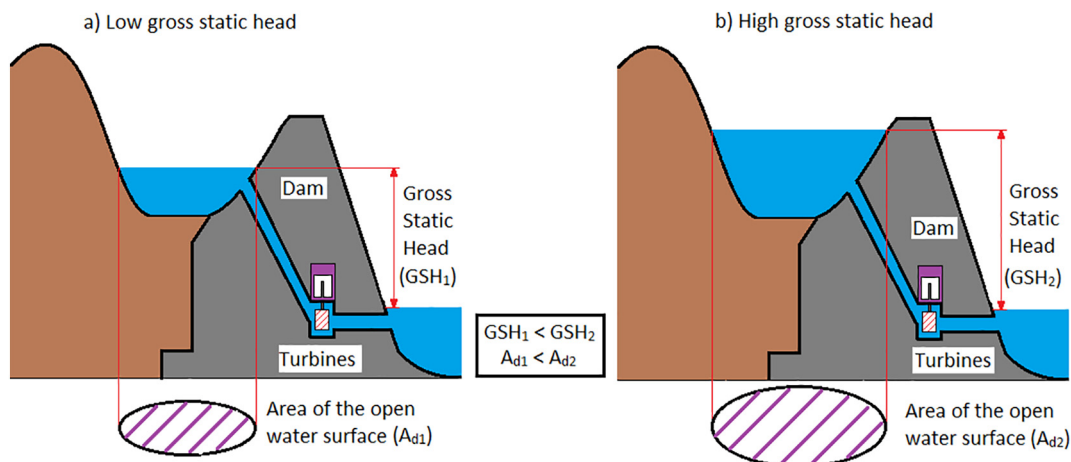

Fig. 2. Relationship between Gross Static Head (GSH) and open water surface area (A_d) where a lower GSH translates into a smaller area.

3.5. Variable dynamics affecting hydropower water footprints

We compared the monthly temporal variation of interlinked variables $Ev_d[r]$ and $A_d[r]$, estimating the effect on electricity production $E_m[p]$, and WFs, $WF_d[p]$.

Step 10 compared the temporal variation of $Ev_d[r]$ and $A_R[r]$ for OWS r per HPP p. Next, **Step 11** compared $WF_d[p]$ (m³) to $E_m[p]$ to assess the relationship between electricity generation and HPP WFs.

3.6. Upscaling the most water-efficient technology

A scenario in which the most water-efficient hydropower plant (MEHP) replaces HPPs in the current Ecuadorian electricity mix, theoretically reduces the WF related to Ecuador's electricity production. Nonetheless, this also affects the electricity system itself and the temporal WF variation, considering only the implications of reservoir water management, excluding infrastructural changes. We assessed the effect of this scenario on the current electricity system in eight steps.

Step 12 estimated the MEHP and **Step 13** monthly electricity generation of a theoretical mix using MEHP technology, $E_m[a]$ (PJ), as:

$$E_m[a] = E_m[MEHP] * f_s \tag{5}$$

where $E_m[MEHP]$ is the monthly $E_m[p]$ for the selected MEHP, and f_s is a scaling factor. For f_s, we assumed that electricity production corresponds to a linear MEHP electricity production increase to provide the current annual electricity production:

$$f_s = \frac{\sum_{m=1}^{12} E_m[c]}{\sum_{m=1}^{12} E_m[MEHP]} \tag{6}$$

Data on $E_m[c]$ consisted of the 2017's monthly electricity production of all on-grid power plants from ARCONEL (2019).

Step 14 calculated monthly WFs, $WF_m[a]$ (m³) per month m, of the theoretical mix of the MEHP technology as:

$$WF_m[a] = WF_m[MEHP] * f_s \tag{7}$$

where, $WF_m[MEHP]$ is the $WF_m[p]$ from **Step 8** per MEHP.

Step 15 calculated the annual WF, $WF_y[a]$ (m³/year) of the mix by aggregating the $WF_m[a]$ to complete a year.

Step 16 compared the $E_m[a]$, the $E_m[c]$, the $WF_y[a]$ and the current annual blue WF of electricity, $WF_y[c]$ (m³).

Step 17 estimated the theoretical monthly electricity generation, $E_m[o]$ (PJ), when the MEHP technology is used in both basins as:

$$E_m[o] = E_m[pac] * f_s[pac] + E_m[ama] * f_s[ama] \tag{8}$$

where $E_m[pac]$ and $f_s[pac]$ refer to the monthly electricity production and the scaling factor of the MEHP in the Pacific basin, and $E_m[ama]$ and $f_s[ama]$ in the Amazon basin. Differences in water availability between the basins cause variation of monthly electricity production and scaling factors. The MEHP determined in **Step 12** is located in only one of the basins. To find temporal variation and electricity output, we used the most similar HPP to the MEHP in the other basin using the inventory of Vaca-Jiménez et al. (2019a). *Appendix D* gives the MEHP selection for the other basin. Data on $E_m[ama]$ and $E_m[pac]$ were derived from ARCONEL (2019).

The theoretical system has the same annual electricity production than the current on-grid electricity mix. We assumed there are HPPs in the two basins, making the definition of $f_s[pac]$ and $f_s[ama]$ more complex. The relationship between them is as follows:

$$f_s[pac] = \frac{\sum_{m=1}^{12} E_m[c]}{\sum_{m=1}^{12} E_m[pac]} = \frac{\sum_{m=1}^{12} E_m[c]}{\sum_{m=1}^{12} E_m[c] - \sum_{m=1}^{12} (E_m[ama]) * f_s[ama]} \tag{9}$$

The definition of $f_s[pac]$ and $f_s[ama]$ was made by an iterative process based on the minimization of the months of the year in which the $E_m[o]$ cannot fulfill the $E_m[c]$. To optimize HPP electricity production, we used the difference in water availability in the basins. *Appendix E* describes the optimization process to assess $f_s[pac]$ and $f_s[ama]$.

Step 18 calculated the WF, $WF_m[o]$ (m³/month) per month m, for the MEHP technology in the Amazon and Pacific basin as:

$$WF_m[o] = WF_{m,e}[pac] * E_m[pac] + WF_{m,e}[ama] * E_m[ama] \tag{10}$$

The case study defines the MEHP from either the Pacific or the Amazon basin. Similarly to **Step 17**, to define the WF of the MEHP in the other basin, we used data of the most similar HPP to the MEHP in the other basin. Thus, either $WF_{m,e}[pac]$ or $WF_{m,e}[ama]$ is the $WF_{m,e}[p]$ defined in **Step 9** for the selected MEHP; the other is derived from Vaca-Jiménez et al. (2019a).

Finally, **Step 19** compared the $E_m[o]$, the $E_m[c]$, and $WF_m[o]$ with the current electricity blue WF per month m, $WF_m[c]$ (m³).

4. Results

4.1. Temporal variation of Open Water Surface size

Fig. 3a–d shows the results of the DEM, giving the annual variation of the OWS sizes of the four HPPs that represent four different hydropower categories. It shows the maximum and minimum surface size based on daily HPP head data from 2008 to 2018. Fig. 3a–d shows the differences between HPPs with *Flooded lakes* (Marcel Laniado and Saucay, Fig. 3a–c) and *Flooded Rivers* (Mazar and Paute, Fig. 3b–d). *Flooded Lakes* have a wider OWS than *Flooded Rivers*. When the size varies, *Flooded Lakes* increase in length and width, covering a larger area. Conversely, as *Flooded Rivers* are constrained by mountains, size variation is mainly seen as an increase of flooded area length rather than width.

Fig. 4a–d shows temporal HPP OWS size variation compared to the areas in the GRanD database (Lehner et al., 2011), and from Vaca-Jiménez et al. (2019a), who used GIS. $DH > GSH$ HPPs show larger temporal OWS size variation than the two $DH < GSH$ HPPs. Marcel Laniado (Fig. 4a) has the largest variation with a more than two-fold difference between the maximum and minimum OWS size. Together, Saucay's reservoirs have the smallest size of the four cases and a 12% difference between the maximum and minimum size.

Fig. 4a–d also shows differences between the OWS' sizes reported in the other databases and the ones estimated in this study. For instance, Fig. 4b and d show that the GRanD's area is smaller than the estimated area in this study, or the one from Vaca-Jiménez et al. (2019a). Fig. 4b and d show that Mazar and Paute's OWSs mostly vary in length. Probably the GRanD database includes OWSs from the dry season, causing the difference, but there is no common trend for all four HPP types.

4.2. Daily evaporation from hydropower open water surfaces

Fig. 5a–d shows differences between HPP OWS evaporation when a variable or constant OWS area is considered. Reservoir evaporation is underestimated for three of the four cases using the *constant approach* (Fig. 5b–d). For Paute ($DH > GSH$ - Flooded river), underestimation is 58 to 72%, for Saucay ($DH < GSH$ - Flooded Lake) 39 to 47%, and for Paute ($DH < GSH$ - Flooded River), 46 to 55%. Underestimation is mainly due to the assumption of previous studies that the OWS is half-full most of the time. For $DH < GSH$ HPPs, if the assumption of a maximum OWS is
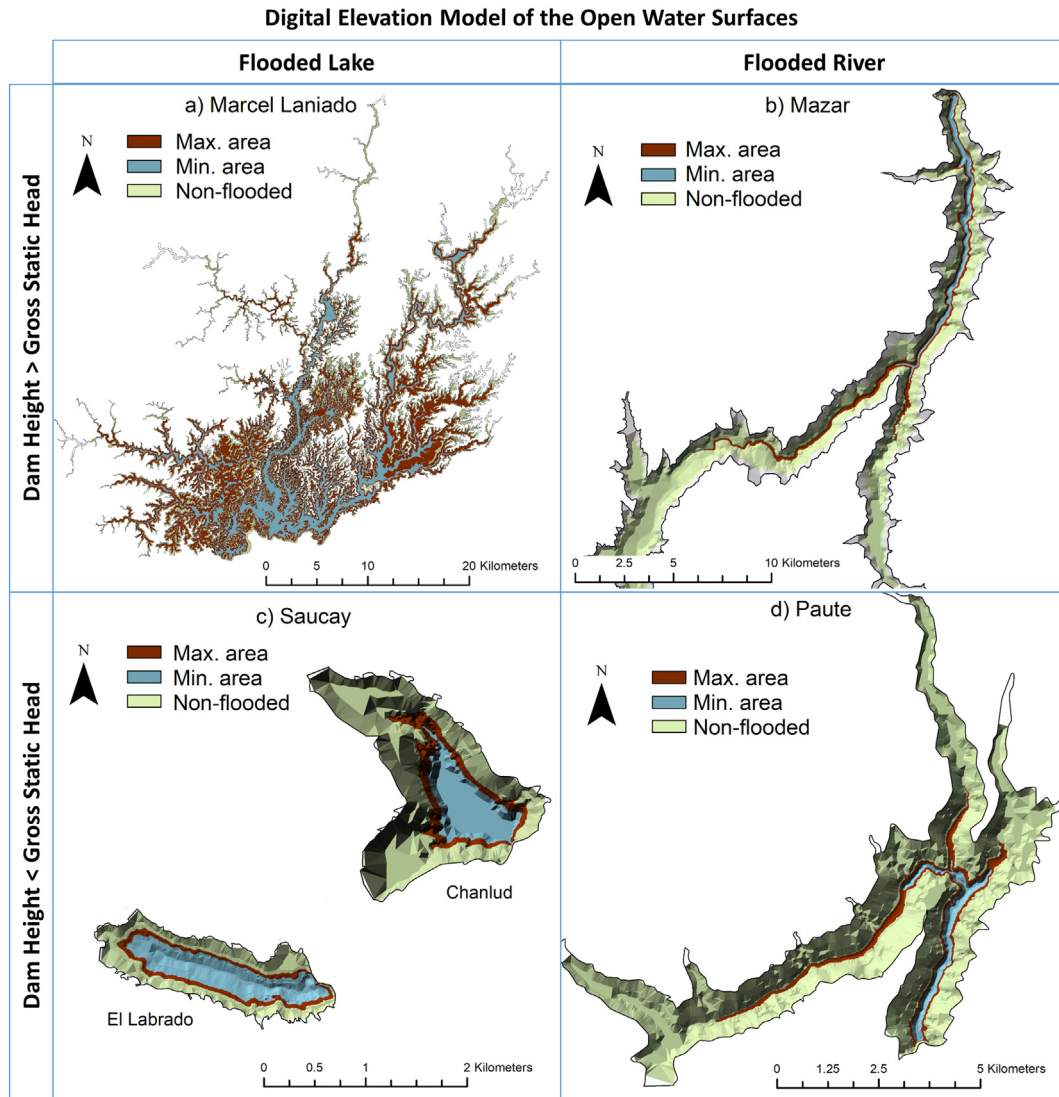
Digital Elevation Model of the Open Water Surfaces

Fig. 3. a–d. Digital elevation model (DEM) of the Open Water Surfaces of the four hydropower plants (HPPs) studied, showing maximum and minimum areas based on daily HPP head data from 2008 to 2018. a) Marcel Laniado hydropower plant (HPP), which Dam height (DH) is larger than its Gross Static Head (GSH), its reservoir forms a Flooded Lake, b) Mazar HPP, DH > GSH, the reservoir forms a Flooded River, c) Saucay HPP, (DH < GSH), with Flooded Lake, and d) Paute HPP, DH < GSH, Flooded river. Note: Saucay hydropower plant has two dams with two non-connected reservoirs: El Labrado and Chanlud.

not considered, the underestimation may be corrected. It seems that for these cases, previous studies that have suggested that considering the reservoir full overestimates WFs are not correct (Hogeboom et al., 2018; Liu et al., 2015; Mekonnen and Hoekstra, 2012). The same cannot be said about *DH > GSH* HPPs. For instance, Marcel Laniado (*DH > GSH - Flooded Lake*), shows a different case as the monthly WF is overestimated (up to 63%) and underestimated (down to 28%) depending on the time of the year.

Fig. 5a–d shows significant evaporation pattern differences between cases. Climate dynamics in relation to the OWS size play a role in evaporation variation. For instance, Marcel Laniado has the largest variation of the four, especially from October to March, also because it has the largest temporal OWS variation. Similarly, Mazar has large evaporation from September to February. Evaporation patterns of *DH < GSH* HPPs are similar for both technologies, but with different magnitudes. Fig. 5a–d also shows large differences between the evaporation of HPPs' OWSs. Marcel Laniado has the largest water volumes evaporated, Saucay the smallest. Despite having both *Flooded Lakes*, the variation is caused by large OWS size differences. The Marcel Laniado's OWS is 400 times larger than Saucay's.

4.3. Water footprints of hydropower plants

Fig. 6a–d shows large monthly blue WF variation per unit of electricity of four groups of hydropower plants. The maximum monthly blue WF of Marcel Laniado is three times larger than the minimum; for Mazar, the maximum is 2.5 times larger than the minimum; for Saucay, the difference is a factor of 1.7 and for Paute 2.4. Fig. 5a–d showed that WF variation is related to OWS evaporation variation. Marcel Laniado has the largest annual evaporation variation, and also the largest WF variation.

Fig. 6a–d also shows that the HPP with the largest monthly and annual blue WFs is Marcel Laniado, followed by Saucay, Mazar, and finally, Paute.

4.4. Variable dynamics affecting hydropower water footprints

Fig. 7a–d shows the temporal variation of the OWS size in relation to reservoir evaporation rates. Marcel Laniado has the largest evaporation rates. This HPPs is the only one in the Ecuadorian lowlands, with higher temperatures, smaller wind speeds, and larger solar radiation levels
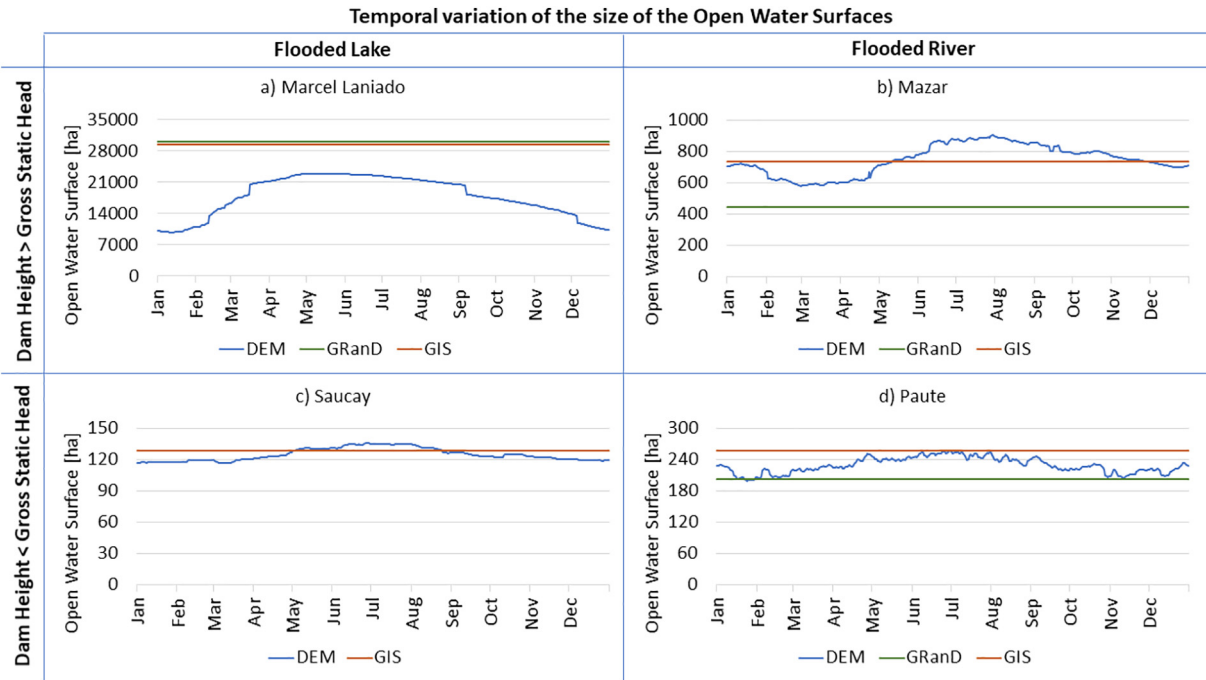
Temporal variation of the size of the Open Water Surfaces

Fig. 4. a–d. Temporal Open Water Surface size variation of four hydropower plants and their relation to the areas in the GRanD database (*Lehner et al., 2011*), and in *Vaca-Jiménez et al.* (2019a) that used Geographic Information Systems (GIS). a) Marcel Laniado hydropower plant (HPP), which Dam height (DH) is larger than its Gross Static Head (GSH), and which reservoir forms a Flooded Lake, b) Mazar HPP, DH > GSH, which reservoir forms a Flooded River, c) Saucay HPP, (DH < GSH), with Flooded Lake, and d) Paute HPP, DH < GSH, Flooded river. Note: Saucay's reservoir does not appear in the GRanD, only in *Vaca-Jiménez et al.* (2019a).

than in the highlands. These climatic factors cause relatively large evaporation rates.

Moreover, Fig. 7c–d shows that for *DH < GSH* HPPs, evaporation is smallest when the OWS area is largest, and vice-versa. The combination of large evaporation and small areas is an expected outcome of a dynamic system, as there is a direct relationship between the dry season and smaller water inputs into the reservoir. However, for *DH > GSH*

HPPs (Fig. 7a–b) the relationship of these factors differs. For Marcel Laniado and Mazar, the largest OWS does not coincide with the smallest evaporation, as there is a delay of over a month. Large surface areas do not always relate to smaller evaporation rates if HPPs decrease their water outflow to store water for dry months, causing a delay of the size-evaporation temporal relationship. Conversely, HPPs with *DH < GSH* do not have this delay as they only store water for a few days.

Daily evaporation from Open Water Surfaces of Hydropower plants
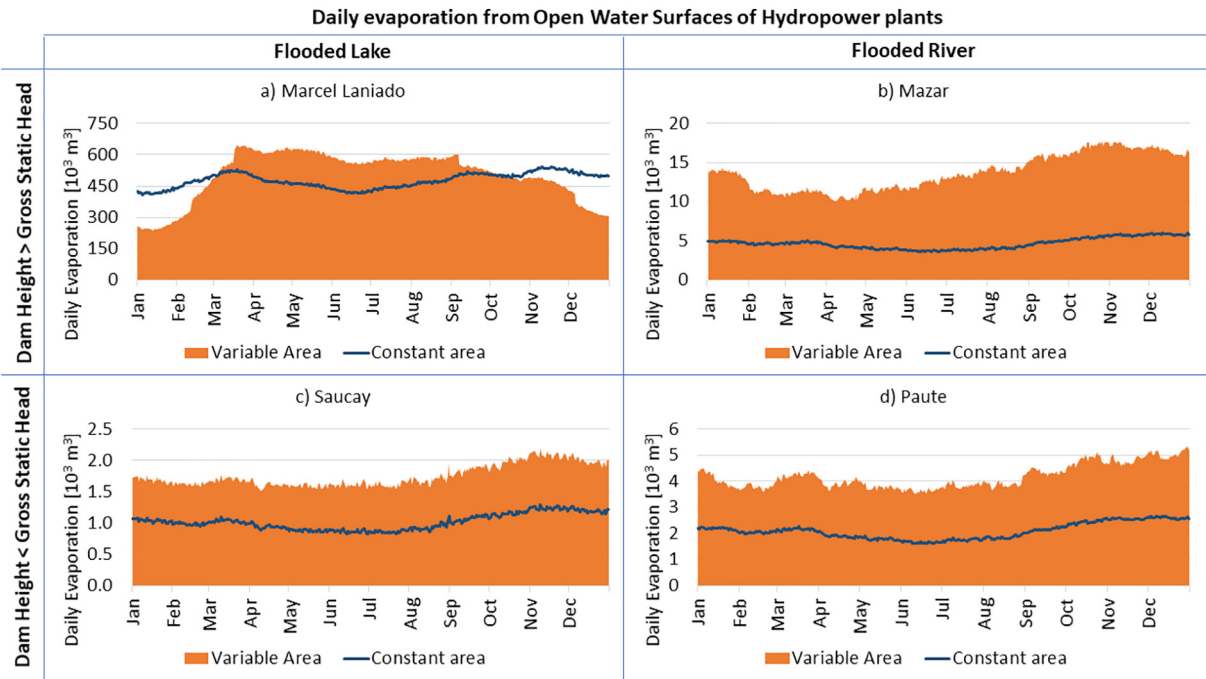

Fig. 5. a–d. Daily Open Water Surface evaporation for four cases considering a variable area or a constant area. a) Marcel Laniado hydropower plant (HPP), which Dam height (DH) is larger than its Gross Static Head (GSH), the reservoir forms a Flooded Lake, b) Mazar HPP, DH > GSH, the reservoir forms a Flooded River, c) Saucay HPP, (DH < GSH), with Flooded Lake, and d) Paute HPP, DH < GSH, with Flooded river.
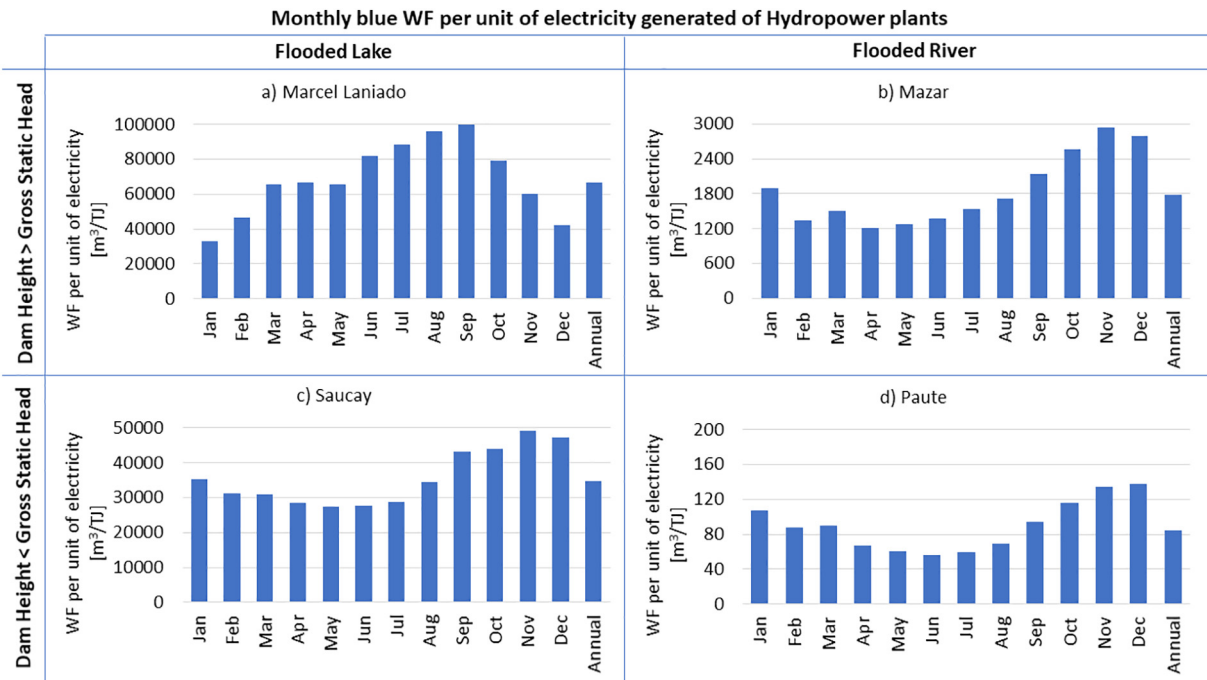
Fig. 6. a–d. Monthly blue WF variation per unit of electricity of four hydropower plants. a) Marcel Laniado hydropower plant (HPP), which Dam height (DH) is larger than its Gross Static Head (GSH), the reservoir forms a Flooded Lake, b) Mazar HPP, DH > GSH, the reservoir forms a Flooded River, c) Saucay HPP, (DH < GSH), with Flooded Lake, and d) Paute HPP, DH < GSH, with Flooded river.

This implies that some HPPs have relatively large OWS areas and significant evaporation rates, translating into relatively large evaporation.

Fig. 8a–d shows the temporal daily OWS evaporation variation and its relationship with the HPP electricity output. The largest electricity output of *DH* < *GSH* HPPs coincide with relatively small *OWS* evaporation (from April to July for Saucay, and from May to July for Paute). This is why these HPPs have the lowest WF in these periods (Fig. 6b–d). However, Fig. 8a–d also shows that for *DH* > *GSH* HPPs with large

storage capacities, electricity output is not inversely related to OWS evaporation. For example, Marcel Laniado has the largest electricity output from March to May. During these periods, its OWS also has relatively large evaporation. From June to August, Mazar experiences a similar effect. *DH* > *GSH* HPP management prioritizes water storage over maximizing electricity output, aiming for more stable electricity output, translating into relatively large WFs during periods with large evaporation. Energy management may have a larger effect on WF dynamics
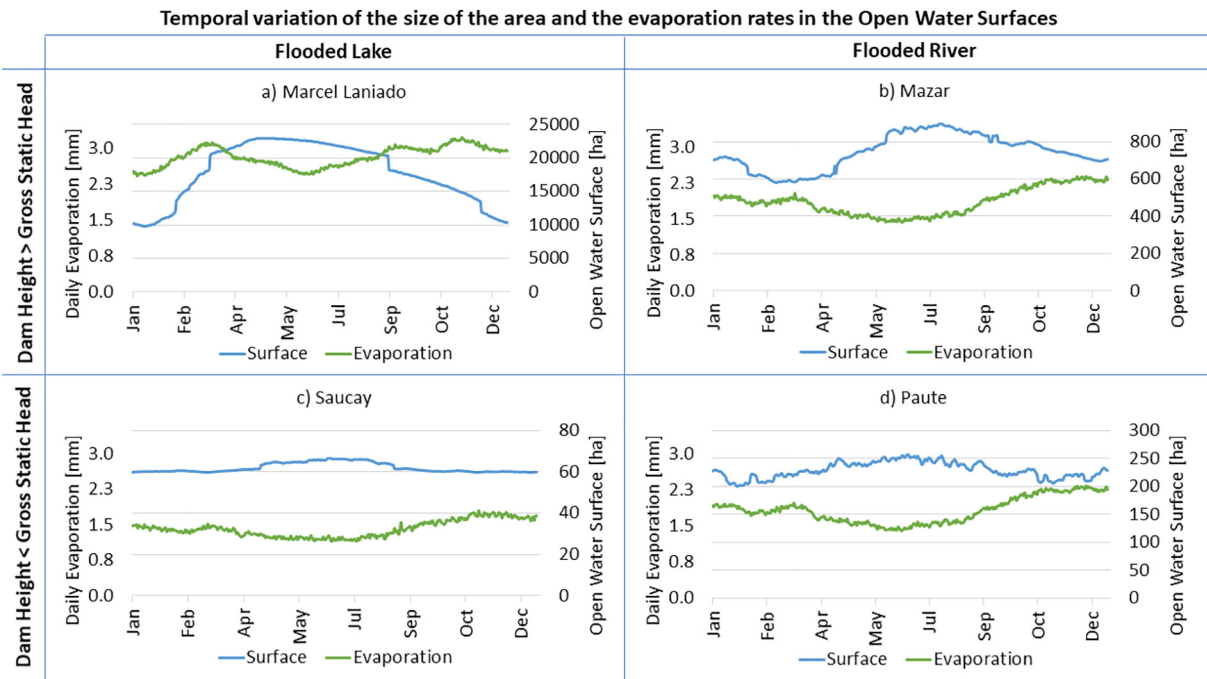

Fig. 7. a–d. Temporal Open Water surface variation and evaporation rates of four types of Ecuadorian Hydropower plants. a) Marcel Laniado hydropower plant (HPP), which Dam height (DH) is larger than its Gross Static Head (GSH), the reservoir forms a Flooded Lake, b) Mazar HPP, DH > GSH, the reservoir forms a Flooded River, c) Saucay HPP, (DH < GSH), with Flooded Lake, and d) Paute HPP, DH < GSH, with Flooded river.
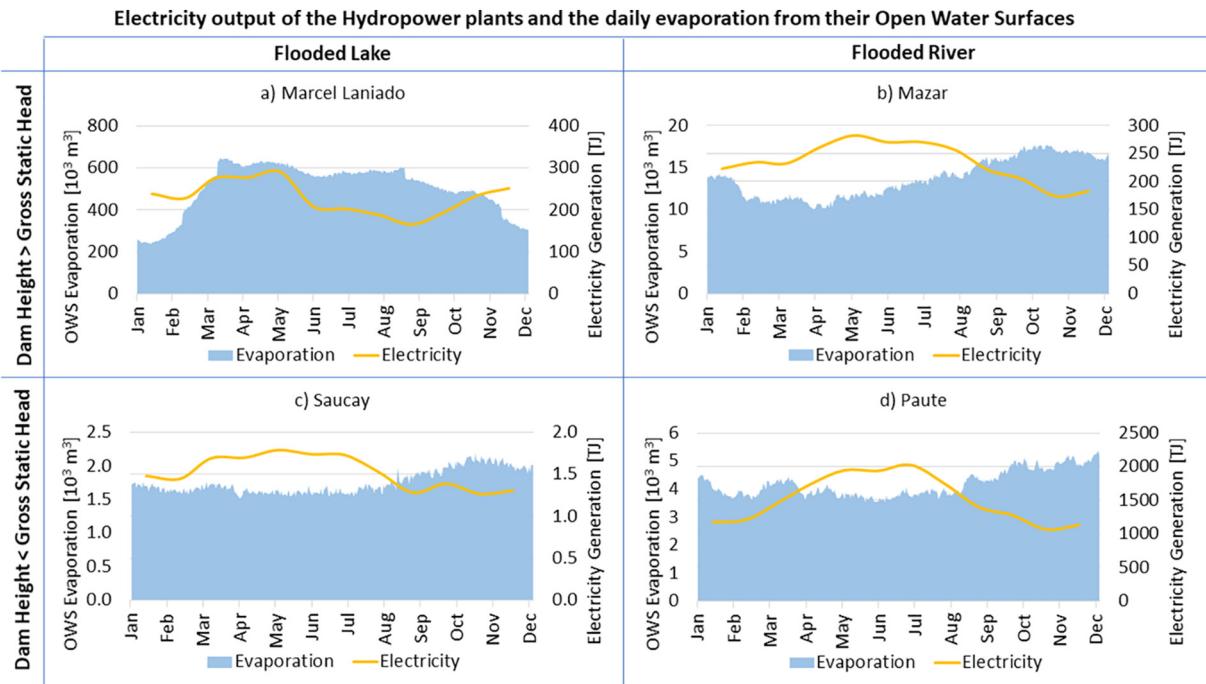
Fig. 8. a–d. Temporal variation of the daily open water surface evaporation and electricity output of four hydropower plants. a) Marcel Laniado hydropower plant (HPP), which Dam height (DH) is larger than its Gross Static Head (GSH), and which reservoir forms a Flooded Lake, b) Mazar HPP, DH > GSH which reservoir forms a Flooded River, c) Saucay HPP, (DH < GSH), with Flooded Lake, and d) Paute HPP, DH < GSH, Flooded river.

than climate variability. Mazar and Paute are situated close to each other and have the same climate. However, the use of the OWS is different. Mazar's reservoir stores water to overcome dry periods, while Paute's reservoir maximizes electricity output, causing different WF dynamics.

Comparing Fig. 8a–d and Fig. 6a–d, differences between the temporal WF variation of the four HPPs becomes clear. Fig. 8a–b shows that the monthly blue WF variation of *DH > GSH* HPPs, observed in Fig. 6a–b, is due to large OWS evaporation variation rather than electricity production variation. WF variation of *DH < GSH* HPPs is due to electricity production variation rather than OWS evaporation variation.

4.5. Upscaling the most water-efficient HPP technology

Paute HPP, in the Amazon basin, have the smallest annual and monthly WFs per unit of electricity generated (Fig. 6a–d), and the second smallest OWS size variation (Fig. 4a–d). Therefore, for this case study, the *DH < GSH, Flooded River* technology is considered as the MEHP.

Fig. 9a–b shows Ecuador's electricity production and its related annual blue WF if the MEHP is scaled up to replace existing HPP infrastructure, and it is deployed in the Amazon basin. Fig. 9b shows that the annual WF of electricity production is reduced to 11% of the current level while providing the same annual amount of electricity. However, Fig. 9a shows that the temporal electricity production variation of this technology (constrained by water availability in the Amazon basin) cannot produce Ecuador's current monthly electricity demand during seven months of the year, from September to March.

Considering water availability variation in the Amazon and Pacific basin, HPPs in the Pacific can back up reduced electricity production in the Amazon during part of its dry season. Fig. 10a–b shows Ecuador's electricity generation and related WF when the MEHP is scaled up to replace existing HPP infrastructure in the two basins. In comparison to Fig. 9a, Fig. 10a shows how *DH < GSH, Flooded River* HPPs in the Pacific
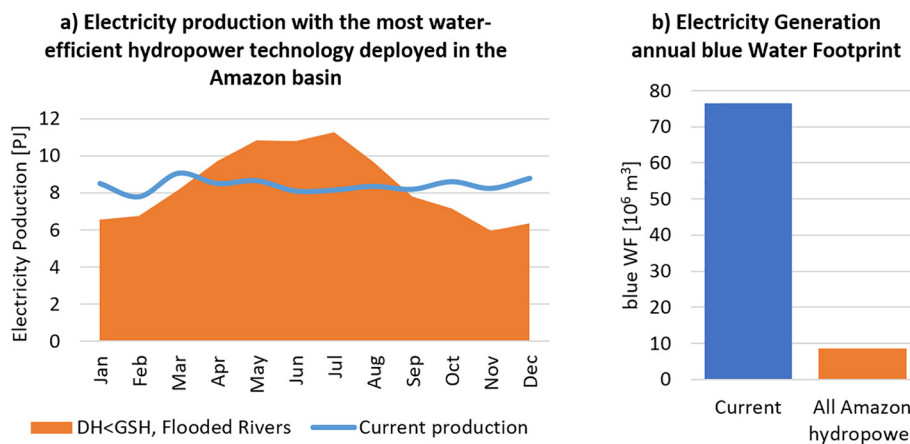

Fig. 9. a–b. Electricity production of Ecuador (a), and its related annual WF (b), if the most water-efficient hydropower technology is scaled up to replace existing infrastructure, and deployed in the Amazon basin. The current case is based on (Vaca-Jiménez et al., 2019b).
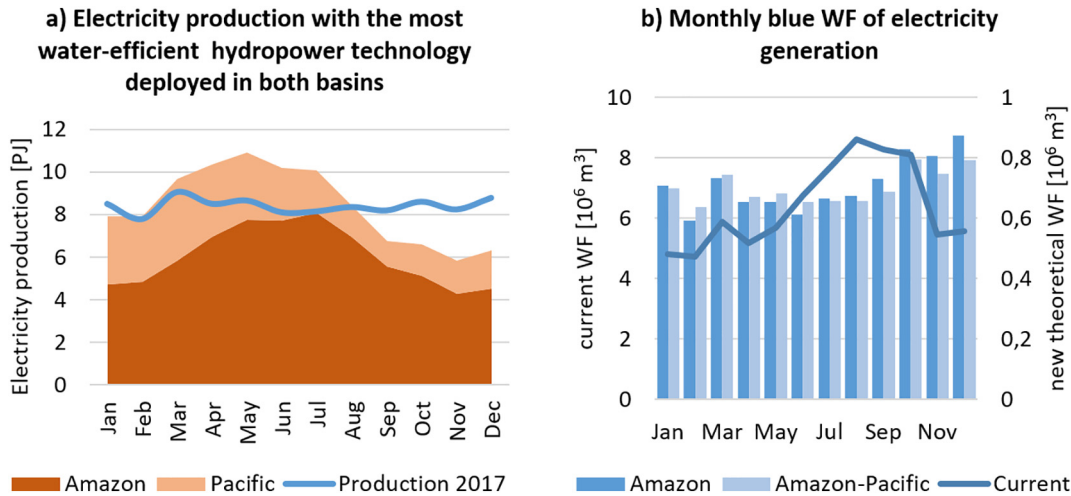
Fig. 10. a–b. Electricity production of Ecuador (a), and its monthly blue WF (b), if the most water-efficient hydropower technology is scaled up to replace the existing infrastructure (including other electricity-generating technologies as thermal power plants) in the Amazon and Pacific basin. Note: The current monthly blue WF is based on Vaca-Jiménez et al. (2019b).

basin could contribute to electricity production and provide electricity for seven months per year, while the total blue electricity WF remains the same (Fig. 10b). Water availability differences between the basins can be used to maximize HPP electricity production throughout the year, although Ecuador still needs other electricity generating technologies to produce sufficient electricity from September to January.

Fig. 10b shows that a shift to *DH < GSH - Flooded River* HPPs implies a change in the WF dynamics of electricity generation as the monthly blue WF variation is smaller than today. This can have beneficial effects on water availability in the country, as there is an offset of electricity as a water competitor from July to October.

5. Discussion

5.1. Implications of open water surfaces variation for WFs

So far, research has excluded HPP OWS size variation, estimating the uncertainty of this assumption using ranges to avoid WF under and overestimation. Our findings suggest that excluding size variation introduces WF underestimations. For Ecuador, the *constant approach* translates into evaporation underestimation of 10 to 80%. Future studies might include temporal variation because water availability and electricity generation are part of a dynamic system. However, the uncertainty of WF estimations of previous studies is not only due to the use of the *constant approach*. Two other factors are:

(i) The assumption that the OWS is half-empty. Previous studies assumed there is a WF overestimation as the OWS temporal variation implied smaller sizes (Herath et al., 2011; Liu et al., 2015; Mekonnen and Hoekstra, 2012). As a response, Hogeboom et al. (2018) introduced a correcting factor for OWS sizes. Our results show that depending on the type of HPP, this assumption might underestimate HPP WFs by half. HPP differences and differences in operation and infrastructure are the reason that generalizations should be made with great care.

(ii) Lack of temporal information in OWS's databases. Sources like the GRanD database give information on HPP OWS sizes and shapes (Lehner et al., 2011), giving average, theoretical and maximum OWS sizes based on different data sources, prioritizing measurements from satellite images. However, in some cases, measurements are based on information for only one day. If satellite images correspond to a day where the OWS size is below average, the size is underestimated, and so is the WF. This is likely the case for Ecuadorian OWS's, as satellite imaging is clearer in the dry season due to fewer clouds. To avoid this bias,

we suggest that future studies measure OWS sizes based on satellite imaging, using pictures from more days, in different years and seasons. In this way, even when the *constant approach* is used, climate and energy planning variables are averaged, reducing uncertainty.

5.2. Energy management and geography influence on WFs

Existing studies have assessed climate and technology effects on HPP WFs (Coelho et al., 2017; Gleick, 1992; Herath et al., 2011; Hogeboom et al., 2018; Liu et al., 2015; Mekonnen and Hoekstra, 2012; Scherer and Pfister, 2016). When system dynamics are also considered, there are two other factors significantly affecting HPP WFs: energy management and geography. Energy management deciding on electricity output and water storage might have a larger effect on temporal evaporation variation than climate. Temporal WF variations of HPPs with relatively large storage are larger than WFs of HPPs with smaller storage. For most HPPs, the goal of water storage is to make power production flexible, especially during dry periods. However, the longer water is stored in the OWS, the larger the evaporation is, causing a tradeoff between reducing WFs or securing a reliable energy supply. Future studies might include this storage-evaporation-electricity generation tradeoff considering temporal variations for a larger range of HPPs storage capacities.

Aiming for small WFs is not necessarily the best option. Previous studies like Coelho et al. (2017), Liu et al. (2015), or Scherer and Pfister (2016), addressed the system from a water management perspective focusing on the effect that HPP reservoirs have on the hydrosphere. Mekonnen et al. (2016) and Mekonnen and Hoekstra (2012), have indicated that it is more efficient to allocate water to water-efficient electricity generating technologies, e.g., wind, solar, or geothermal power plants. Bakken et al. (2016a), Gleick (1992) and Vaca-Jiménez et al. (2019a) have shown that there are less water-intensive HPP technologies, e.g., RORs with smaller WFs per unit of electricity than HPPs with *Flooded Lakes*. All studies favored the smallest WF. However, when the electricity perspective is included, and energy management is considered, the smallest WFs do not always go along with the best technology and do not guarantee sufficient and reliable electricity production. One of the main advantages of HPPs compared to other renewable energy technologies is their storage, which is paramount for a transition towards low-carbon electricity generation (Soria et al., 2015). The discussion should not focus merely on the best water-efficiency but consider both energy and water perspectives to suggest pathways forward.

Geography also has an important role in OWS water evaporation variation. HPPs in between mountains have deeper and narrower flooded areas, resulting in smaller WFs (Liu et al., 2015; Vaca-Jiménez et al., 2019a). We also found this effect on the OWS temporal WF variation. When the flooded area varies throughout the year, it is limited by the geography, and therefore, the size change is smaller than for HPPs in the highlands or lowlands with shallow and wide flooded areas.

5.3. Results in the context of other assessment methods

Besides the Gross WF method used in this study, there are three other methods to estimate HPP WFs: (i) The Net WF method, relating evaporation and electricity output, like the Gross WF, but considering evaporation differences before and after HPP construction (e.g., Bakken et al. (2016a) and Herath et al. (2011)). (ii) The Water Balance WF method, considering reservoir water input-output and electricity output, e.g., Coelho et al. (2017) and Herath et al. (2011), assuming precipitation cached by the reservoir is the input and evaporation the output. And (iii) the Scarcity WF method, considering a reservoir water balance, including evaporation differences between pre- and post-HPP construction, relating to available water flows at the HPP location, e.g., Scherer and Pfister (2016).

Different methods to calculate the WF serve different purposes. We used the Gross Method as it relates water evaporation and electricity output directly, permitting us to use available data and to compare our results with results from earlier studies that used the same method but were based on the OWS *constant approach*. Despite the method used, OWS evaporation determines HPP WFs, and therefore, the comparison of results is not limited to studies based on the Gross Method only. We have shown that OWS evaporation has large temporal variation due to the dynamics between the operational and climate factors of the HPP. Our study contributes to a better understanding of the OWS temporal variation, energy management, and WFs.

Our study also shows how OWS temporal variation affects WF values estimated by other methods. For instance, OWS temporal variation will likely affect results from the Water Balance and the Water Scarcity method in a similar way, because precipitation water input of the system will also vary. The larger the OWS, the larger the precipitation captured, and vice-versa. Interesting dynamics may emerge between the temporal variation of water input and output using these methods when OWS variation is considered. OWS temporal variation will also affect the Net method because the temporal OWS size variation implies a change in the pre-flooding area considered, indicating that there is a constant land-use change by reservoir areas that flood seasonally. The comparison between methods considering the temporal variation of the OWS should be addressed in future studies.

5.4. Limitations of the study

We grouped Ecuadorian dammed HPPs into four classes, which cover a large range of possible physical and operational HPP conditions. The findings do not represent all HPPs in the global electricity mix due to climate and infrastructure differences. Our results reflect HPPs in countries with equatorial and subtropical climates, e.g., in Colombia, Brazil, or Peru. Countries in higher latitudes or with different climates may have different relations between water storage, climate, and WFs. In some countries, temporal climate variation is more extreme than in Ecuador (WATCH, 2019), with a larger effect on temporal WF variation than water storage. Future studies might use similar approaches to assess HPP WFs for different climates. The study only assessed four cases (one per class). Future studies might include other cases to assess ranges and trends.

The major limitation of this study is the estimation of the DEM of the OWS because there are uncertainties in data precision, especially for areas flooded most of the year. We assumed this uncertainty is not significant, as it might affect the OWS water volume estimation more than

the area size. Another limitation was the lack of daily electricity production data per power plant. This hindered the possibility of making daily WF assessments per unit of electricity produced.

Finally, the simple scenario analysis showing MEHP impact on the electricity system and WF is theoretical and excludes complexities involved in energy management, the feasibility of resources, or infrastructure change. This simplification may be practically unfeasible but helps to show the implications of aiming for the smallest WF constructing HPPs that do not use their full OWS storage capacity. The smallest WF scenario shows the storage-evaporation-electricity generation tradeoff.

6. Conclusions

This study assessed WFs of four different groups of hydropower plants, considering the temporal variation of Open Water Surface sizes, using a Digital Elevation Model and historical data of *Gross Static Heads*. There are large differences among HPP WFs. Important factors include variation of climate, electricity production, and Open Water Surface size. HPP operation management, geographical features, and local climate determine temporal differences, defining the system dynamics. Excluding Open Water Surface sizes causes an underestimation of the annual WF by 10% for HPPs with Flooded Lakes, to 80% for HPPs with Flooded Rivers.

The larger the storage capacity, the larger is the evaporation from the HPP reservoir due to the combination of low electricity output, relatively large evaporation rates, and large reservoir size. Counterintuitively, there is a need to reduce HPP storage capacity to reduce water consumption. This brings an additional tradeoff to consider in the discussion about the possible energy transition paths, as storage capacity is one of the factors that make hydropower more advantageous over other renewable technologies, such as solar or wind. HPPs with dam heights below the *Gross Static Head*, and OWSs forming a *Flooded River* are the most water-efficient hydropower technologies because water storage is limited and evaporation losses relatively small. However, when this technology is scaled-up to replace the current Ecuadorian hydropower infrastructure, the lack of water storage translates into the impossibility to fulfill current electricity production. Although this technology is less water-intensive, its electricity production depends on water availability, and therefore, it lacks flexibility. The system dynamics suggest that the aim for the smallest WF is not always the best option from an energy and water perspective. Despite hydropower consumes water, it is a renewable energy technology that has the advantage that it can store energy so that it might have a role in the future energy mix.

References

ARCONEL, 2018. Estadística anual y multianual del sector eléctrico ecuatoriano 2017 (Quito).

ARCONEL, 2019. SISDAT-BI: Reportes de Información Estadística del Sector Eléctrico (Quito).

Bakken, T.H., Killingtveit, Å., Engeland, K., Alfredsen, K., Harby, A., 2013. Water consumption from hydropower plants - review of published estimates and an assessment of the concept. Hydrol. Earth Syst. Sci. 17, 3983–4000. https://doi.org/10.5194/hess-17-3983-2013.

Bakken, T.H., Modahl, I.S., Engeland, K., Raadal, H.L., Arnoy, S., 2016a. The life-cycle water footprint of two hydropower projects in Norway. J. Clean. Prod. 113, 241–250. https://doi.org/10.1016/j.jclepro.2015.12.036.

Bakken, T.H., Modahl, I.S., Raadal, H.L, Bustos, A.A., Arnoy, S., 2016b. Allocation of water consumption in multipurpose reservoirs. Water Policy 18, 932–947. https://doi.org/10.2166/wp.2016.009.

Cai, X., Wallington, K., Shafiee-Jood, M., Marston, L., 2018. Understanding and managing the food-energy-water nexus – opportunities for water resources research. Adv. Water Resour. 111, 259–273. https://doi.org/10.1016/j.advwatres.2017.11.014.

CELEC EP - Hidronación, 2013. 25 Años presa Daule-Peripa 1988–2013. Imprenta Monsalve Moreno, Guayaquil.

CELEC EP - Hidronación, 2014. Operación conjugada daule peripa-baba: Año 2014 (Guayaquil).

CELEC EP - Hidronación, 2018. Información Técnica [WWW document]. https://www.celec.gob.ec/hidronacion/, Accessed date: 23 June 2018.

CELEC EP - Hidropaute, 2018. Centrales [WWW document]. https://www.celec.gob.ec/hidropaute/#, Accessed date: 23 June 2018.

CEPAL, 2010. Diagnóstico de las Estadísticas del Agua en Ecuador.

Coelho, C.D., Da Silva, D.D., Sediyama, G.C., Moreira, M.C., Pereira, S.B., Lana, Â.M.Q., 2017. Comparison of the water footprint of two hydropower plants in the Tocantins River Basin of Brazil. J. Clean. Prod. 153, 164–175. https://doi.org/10.1016/j.jclepro.2017.03.088.

Coelho, C.D., da Silva, D.D., Sediyama, G.C., Moreira, M.C., Pereira, S.B., Lana, Â.M.Q., 2018. Estimates of monthly and annual evaporation rates and evaporated volumes per unit time in the Tucuruí-pa and Lajeado-to hydroelectric power plant reservoirs based on different methods. Eng. Agric. 38, 38–46. https://doi.org/10.1590/1809-4430-Eng.Agric.v38n1p38-46/2018.

CONELEC, 2008. Atlas solar del ecuador, Conelec (Quito).

Egré, D., Milewski, J.C., 2002. The diversity of hydropower projects. Energy Policy 30, 1225–1230. https://doi.org/10.1016/S0301-4215(02)00083-6.

Elecaustro, 2018. Centrales y Represas [WWW document]. http://www.elecaustro.com.ec/index.php?option=com_content&view=featured&Itemid=281, Accessed date: 23 June 2018.

Gleick, P.H., 1992. Environmental consequences of hydroelectric development: the role of facility size and type. Energy 17, 735–747. https://doi.org/10.1016/0360-5442(92)90116-H.

Gleick, P.H., 1994. Water and energy. Annu. Rev. Energy Environ. 19, 267–299.

Grubert, E.A., 2016. Water consumption from hydroelectricity in the United States. Adv. Water Resour. 96, 88–94. https://doi.org/10.1016/j.advwatres.2016.07.004.

Harwell, G.R., 2012. Estimation of evaporation from open water - a review of selected studies, summary of U.S. Army Corps of Engineers data collection and methods, and evaluation of two methods for estimation of evaporation from five reservoirs in Texas. U.S. Geological Survey Scientific Investigations Report 2012–5202. Denver, Colorado.

Herath, I., Deurer, M., Horne, D., Singh, R., Clothier, B., 2011. The water footprint of hydroelectricity: a methodological comparison from a case study in New Zealand. J. Clean. Prod. 19, 1582–1589. https://doi.org/10.1016/j.jclepro.2011.05.007.

Hoekstra, A.Y., Chapagain, A.K., Aldaya, M.M., Mekonnen, M.M., 2011. The Water Footprint Assessment Manual. 1st ed. Earthscan, London.

Hogeboom, R.J., Knook, L., Hoekstra, A.Y., 2018. The blue water footprint of the world's artificial reservoirs for hydroelectricity, irrigation, residential and industrial water supply, flood protection, fishing and recreation. Adv. Water Resour. 113, 285–294. https://doi.org/10.1016/j.advwatres.2018.01.028.

ICOLD, 2018. ICOLD's World Register of Dams [WWW document]. http://icold-cigb.net/GB/world_register/world_register_of_dams.asp, Accessed date: 25 February 2018.

IEA, 2016. World Energy Outlook 2016. IEA publications, Paris https://doi.org/10.1787/weo-2016-en.

IGM, 2018. Cartografía Básica Oficial.

INAMHI, 2018. Meteorologia [WWW document]. http://www.serviciometeorologico.gob.ec/, Accessed date: 4 May 2018.

INAMHI, 2019. Geoinformación Hidrometeorológica [WWW document]. http://www.serviciometeorologico.gob.ec/geoinformacion-hidrometeorologica/, Accessed date: 1 January 2019.

Kumar, A., Schei, T., Ahenkorah, A., Caceres Rodriguez, R., Devernay, J.-M., Freitas, M., Hall, D., Killingtveit, Å., Liu, Z., 2011. Hydropower. In: Edenhofer, O., Pichs-Madruga, R., Sokona, Y., Seyboth, K., Matschoss, P., Kadner, S., Zwickel, T., Eickemeier, P., Hansen, G., Schlömer, C., von Stechow, C. (Eds.), IPPC Special Report on Renewable Energy Sources and Climate Change Mitigation. Cambridge University Press, Cambridge, UK and New York, USA, pp. 437–496.

Lehner, B., Liermann, C.R., Revenga, C., Vorosmarty, C., Fekete, B., Crouzet, P., Doll, P., Endejan, M., Frenken, K., Magome, J., et al., 2011. Global Reservoir and Dam Database, Version 1 (GRanDv1): Dams, Revision 01. NY NASA Socioecon. Data Appl. Cent, Palisades.

Liu, J., Zhao, D., Gerbens-Leenes, P.W., Guan, D., 2015. China's rising hydropower demand challenges water sector. Sci. Rep. 5, 11446. https://doi.org/10.1038/srep11446.

MEER, 2017. Plan Maestro de Electricidad 2016–2025 (Quito).

Mekonnen, M.M., Hoekstra, A.Y., 2012. The blue water footprint of electricity from hydropower. Hydrol. Earth Syst. Sci. 16, 179–187. https://doi.org/10.5194/hess-16-179-2012.

Mekonnen, M.M., Gerbens-Leenes, P.W., Hoekstra, A.Y., 2015. The consumptive water footprint of electricity and heat: a global assessment. Environ. Sci. Water Res. Technol 1, 285–297. https://doi.org/10.1039/c5ew00026b.

Mekonnen, M.M., Gerbens-Leenes, P.W., Hoekstra, A.Y., 2016. Future electricity: the challenge of reducing both carbon and water footprint. Sci. Total Environ. 569, 1282–1288. https://doi.org/10.1016/j.scitotenv.2016.06.204.

Rollenbeck, R., Bendix, J., 2011. Rainfall distribution in the Andes of southern Ecuador derived from blending weather radar data and meteorological field observations. Atmos. Res. 99, 277–289. https://doi.org/10.1016/j.atmosres.2010.10.018.

Scherer, L., Pfister, S., 2016. Global water footprint assessment of hydropower. Renew. Energy 99, 711–720. https://doi.org/10.1016/j.renene.2016.07.021.

SENAGUA, 2002. Cuencas hidrograficas del Ecuador. Serv. Geoinformacion.

Snyder, D.T., Haluska, T.L., Respini-Irwin, D., 2013. The Shoreline Management Tool—An ArcMap Tool for Analyzing Water Depth, Inundated Area, Volume, and Selected Habitats, With an Example for the Lower Wood River Valley, Oregon (Oregon).

Soria, R., Portugal-Pereira, J., Szklo, A., Milani, R., Schaeffer, R., 2015. Hybrid concentrated solar power (CSP)–biomass plants in a semiarid region: a strategy for CSP deployment in Brazil. Energy Policy 86, 57–72. https://doi.org/10.1016/j.enpol.2015.06.028.

Vaca-Jiménez, S., Gerbens-Leenes, P.W., Nonhebel, S., 2019a. The water footprint of electricity in Ecuador: technology and fuel variation indicate pathways towards water-efficient electricity mixes. Water Resour. Ind. 22, 100112. https://doi.org/10.1016/j.wri.2019.100112.

Vaca-Jiménez, S., Gerbens-Leenes, P.W., Nonhebel, S., 2019b. Water-electricity nexus in Ecuador: the dynamics of the electricity's blue water footprint. Sci. Total Environ. 696, 133959. https://doi.org/10.1016/j.scitotenv.2019.133959.

WATCH, 2019. Evaporation in average year (1985–1999) [WWW document]. http://www.waterandclimatechange.eu/evaporation/average-monthly-1985-1999, Accessed date: 4 August 2019.

Glossary

DH: dam height, considered from the base to the top of the dam (in m)
DEM: digital Elevation Model. 3D model of the open water surface
HPP: hydropower plant
GSH: Gross Static Head (in m). The vertical distance from the open water surface to the top of the water in the tailrace (at the discharge)
MEHP: most water-efficient hydropower plant
ROR: run-of-the-river hydropower plants
OWS: Open Water Surface
WF: water footprint